SECURITY AND COMMUNICATION NETWORKS
Security Comm. Networks 2013; **6**:1301–1309
Published online 14 February 2013 in Wiley Online Library (wileyonlinelibrary.com). DOI: 10.1002/sec.712

RESEARCH ARTICLE

Generation of potential wells used for quantum codes transmission via a TDMA network communication system

Iraj Sadegh Amiri[1]*, Mehrnaz Nikmaram[2], Ali Shahidinejad[2] and Jalil Ali[1]

[1] Institute of Advanced Photonics Science, Nanotechnology Research Alliance, Universiti Teknologi Malaysia (UTM), Johor Bahru, 81310, Malaysia
[2] Faculty of Computer Science and Information Systems (FCSIS), Universiti Teknologi Malaysia (UTM), Johor Bahru, 81300, Malaysia

ABSTRACT

This paper proposes a technique of quantum code generation using optical tweezers. This technique uses a microring resonator made of nonlinear fibre optics to generate the desired results, which are applicable to Internet security and quantum network cryptography. A modified add/drop interferometer system called PANDA is proposed, which consists of a centred ring resonator connected to smaller ring resonators on the left side. To form the multifunction operations of the PANDA system—for instance, to control, tune and amplify—an additional Gaussian pulse is introduced into the add port of the system. The optical tweezers generated by the dark soliton propagating inside the PANDA ring resonator system are in the form of potential wells. Potential well output can be connected to the quantum signal processing system, which consists of a transmitter and a receiver. The transmitter is used to generate high-capacity quantum codes within the system, whereas the receiver detects encoded signals known as quantum bits. Therefore, an entangled photon pair can be generated and propagated via an optical communication link such as a time division multiple access system. Here, narrower potential wells with a full-width half-maximum of 3.58 and 9.57 nm are generated at the through and drop ports of the PANDA ring resonator system, respectively, where the amplification of the signals occurs during propagation inside the system.

KEYWORDS

Internet security; optical potential wells; quantum cryptography; time division multiple access; entangled photon pair

***Correspondence**

Iraj Sadegh Amiri, Institute of Advanced Photonics Science, Nanotechnology Research Alliance, Universiti Teknologi Malaysia (UTM), 81310 Johor Bahru, Malaysia.
E-mail: isafiz@yahoo.com

1. INTRODUCTION

In optical communication, dark Gaussian soliton controls within a semiconductor add/drop multiplexer have numerous applications [1]. Microring resonators (MRRs) are types of Fabry–Pérot resonators, which can be readily integrated in array geometries for useful functions in areas such as optical communication, signal processing and network security in the nanoscale regime. Its nonlinear phase response can also be readily incorporated into an interferometer system to produce a specific intensity output function [2]. One interesting result emerges through the use of a PANDA ring resonator [3], which is a good candidate for nanoscale interferometer applications. One new feature of this specific model of ring resonator, which introduces a system of nanoscale-sensing transducers based on the PANDA ring resonator, was presented by Tamee *et al*. [4]. Amiri *et al*. have shown that the multisoliton can be generated and controlled within a PANDA ring resonator and add/drop filter systems, in which ultra-short multiple dark-bright solitons with a full-width half-maximum (FWHM) of 425 pm and free spectrum range of 1.145 nm, respectively, were generated [5].

The optical tweezers technique is recognized as a powerful tool for the manipulation of micrometre-sized particles in three spatial dimensions. In many research areas, optical tweezers are used to store and trap light, atoms, molecules or particles within the proposed system. This technique, which has widespread applications in the biological and physical sciences [6], has the unique ability to trap and manipulate molecules at mesoscopic scale. The output is achieved when the high optical field is set up with an optical tweezers apparatus [7].

Within the PANDA ring resonator system, tweezers are kept stable in the form of valleys or potential wells. Moreover, it has been shown that the transferring of trapped atoms between two optical potentials can be performed in this system [8]. Several emerging technologies, such as integrated all-optical signal processing and all-optical quantum information processing, require interactions between two distinct optical signals. Optical tweezers tools can be used to trap molecules or photons [9].

Because security has become an important issue for modern Internet service, one security technique that has been widely used and investigated in many applications is known as quantum cryptography, which uses optical tweezers [10]. Yupapin *et al.* [11] have proposed a new technique for quantum key distribution, which can be used for communication transmission security. It also can be implemented with a small device, such as a mobile telephone handset. Similarly, Mitatha *et al.* [12] have designed a new method of secure packet switching, which uses nonlinear behaviours of light in MRR, which can be used for high-capacity transmission and security switching. Recently, quantum networks have shown promise for the creation of ideal network security [13]. To date, quantum key distribution is the only form of information that can do so. Yupapin *et al.* [14] have shown that a continuous wavelength can be generated by using a soliton pulse in an MRR. The secret key codes are generated via an entangled photon pair, which is used for security purposes via dark soliton pulse propagation.

In this study, a PANDA ring resonator system, which consists of an add/drop interferometer system connected to a small ring resonator on the left side, is used. This system can be applied to generate nano-sized bandwidth peaks of optical tweezers in the form of potential wells; these can generate a large amount of quantum codes propagating inside the network communication link, for example, in a time division multiple access (TDMA) system. In this system, several stations connected to the same physical medium—for example, those sharing the same frequency channel—can communicate. TDMA is a channel access method for shared medium networks in which the users receive information in different time slots. TDMA can also be used in digital mobile communications and satellite systems, where highly secure signals of quantum user codes can be transmitted using a coding method such as Manchester. This technique has advantages because of its low duty cycle and high power efficiency compared with other techniques such as wavelength division multiple access or frequency division multiple access, which makes TDMA the preferred option for applications involving portable devices where power consumption is critical. Therefore, security can be assured through both a nano-bandwidth pulse generation system—namely, a PANDA ring resonator, which has undetectable pulses—and the transmitter system known as TDMA, which transmits secret codes. The security of these systems is established through the generation of ultra-short pulses along the ring system and the transmission of secret codes.

2. THEORETICAL MODELLING

The methodology used is based on solving the nonlinear equation of interferometer PANDA ring resonator systems, which can be implemented in the simulation method by inserting practical system parameters. Therefore, the nonlinear equation of propagating a signal inside the fibre optic interferometer PANDA ring resonator is presented in order to simulate ultra-short output signals to be used in secured communication networks. The dark soliton pulse is introduced into the PANDA ring resonator system, as shown in Figure 1. Dark soliton has a unique property, in which the soliton amplitude vanishes during propagation in various media [15]. Dynamic behaviour of the optical tweezers appears when the Gaussian beam is added into the add port of the system [16]. The dark and Gaussian beams propagate inside the system with a central wavelength of $\lambda_0 = 1.55\ \mu m$.

Input optical fields of the dark soliton (E_{i1}) and the Gaussian pulse (E_{i2}) are expressed in Equations (1) and (2) [17].

$$E_{i1}(t,z) = A \tanh\left[\frac{T}{T_0}\right] \exp\left[\left(\frac{z}{2L_D}\right) - i\omega_0 t\right] \quad (1)$$

$$E_{i2}(t,z) = E_0 \exp\left[\left(\frac{z}{2L_D}\right) - i\omega_0 t\right] \quad (2)$$

A and z are the optical field amplitude and propagation distance, respectively. T is a soliton pulse propagation time in a frame moving at the group velocity, $T = t - \beta_1 \times z$, where β_1 and β_2 are the coefficients of the linear and second-order terms of Taylor's expansion of the propagation constant [18]. $L_D = T_0^2/|\beta_2|$ is the dispersion length of the soliton pulse. The frequency carrier of the soliton is ω_0. Soliton is realized as a pulse that keeps its temporal width invariance as it propagates and thus is known as temporal soliton [19]. Soliton peak intensity is $\left(|\beta_2/\Gamma T_0^2|\right)$. Here, $\Gamma = n_2 \times k_0$ is the length scale, over which dispersive or nonlinear effects make the beam become wider or narrower. For the temporal soliton pulse in the microring device, a balance should be achieved between the dispersion length (L_D) and the nonlinear length ($L_{NL} = (1/\gamma\varphi_{NL})$, where γ and φ_{NL} are the coupling loss of the field amplitude and nonlinear phase shift; thus, $L_D = L_{NL}$ [20]. Light propagates within the nonlinear medium, wherein the refractive index (n) is given by the following:

$$n = n_0 + n_2 I = n_0 + \left(\frac{n_2}{A_{eff}}\right) P \quad (3)$$

In Equation (3), n_0 and n_2 are the linear and nonlinear refractive indexes, respectively. I and P represent the optical intensity and optical power, respectively. The effective mode core area of the device is given by A_{eff} [21]. In Figure 1, the resonant output is formed; thus, the normalized output of the light field is the ratio between the output and input fields $E_{out}(t)$ and $E_{in}(t)$. The output and input signals in each round trip of a single ring resonator is given in Equation (4):

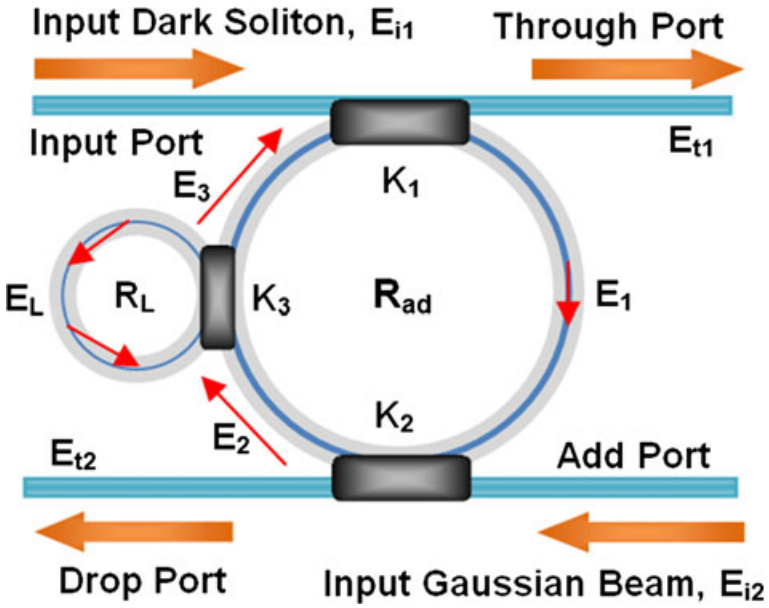

Figure 1. A schematic diagram of a PANDA ring resonator system.

$$\left|\frac{E_{\text{out}}(t)}{E_{\text{in}}(t)}\right|^2 = (1-\gamma)\left[1 - \frac{(1-(1-\gamma)x^2)\kappa}{\left(1-x\sqrt{1-\gamma}\sqrt{1-\kappa}\right)^2 + 4x\sqrt{1-\gamma}\sqrt{1-\kappa}\sin^2\left(\frac{\phi}{2}\right)}\right] \tag{4}$$

The closed form of Equation (4) indicates that this ring resonator is comparable with a Fabry–Pérot cavity. It has input and output mirrors with field reflectivity $(1-\kappa)$ and a fully reflecting mirror. Here, κ is the coupling coefficient, and $x = \exp(-\alpha L/2)$ represents a round-trip loss coefficient; $\varphi_0 = kLn_0$ and $\varphi_{\text{NL}} = kLn_2|E_{\text{in}}|^2$ are the linear and nonlinear phase shifts; $k = 2\pi/\lambda$ is the wave propagation number in a vacuum. L and α are a waveguide length and linear absorption coefficient, respectively [22]. In this study, an iterative method is inserted to obtain the needed results by using Equation (4). Interior signals of the PANDA ring resonator system are given by the following:

$$E_1 = \sqrt{1-\gamma_1} \times \left[E_3 \times \sqrt{1-\kappa_1} + j\sqrt{\kappa_1} \times E_{i1}\right] \tag{5}$$

$$E_2 = \sqrt{1-\gamma_2} \times \left[E_1 \times \sqrt{1-\kappa_2} + j\sqrt{\kappa_2} \times E_{i2}\right] \tag{6}$$

$$E_3 = E_L \times E_2 \times e^{\frac{-\alpha L}{4} - jk_n\frac{L}{2}} \tag{7}$$

$$E_L = E_2 \times \left\{\frac{\sqrt{(1-\gamma_3)\times(1-\kappa_3)} - (1-\gamma_3)\times e^{\frac{-\alpha}{2}L_L - jk_nL_L}}{1-\sqrt{(1-\gamma_3)\times(1-\kappa_3)}\times e^{\frac{-\alpha}{2}L_L - jk_nL_L}}\right\}. \tag{8}$$

κ is the coupling coefficients, and the ring resonator loss is α. The fractional coupler intensity loss is γ. The circumferences of the centred and left rings are $L = 2\pi R_{\text{ad}}$ and $L_{\text{L}} = 2\pi R_{\text{L}}$, respectively, where R and R_{L} are the radii of the rings. Two complementary optical circuits of the PANDA ring resonator system, E_{t1} and E_{t2}, can be expressed by Equations (9) and (10):

$$E_{t1} = -C_1C_2y_2\sqrt{\kappa_1}E_{i2}e^{-\frac{\alpha L}{2} - jk_n\frac{L}{2}} + \left[\frac{C_2C_3\kappa_1\sqrt{\kappa_2}E_LE_{i1}\left(e^{-\frac{\alpha L}{2} - jk_n\frac{L}{2}}\right)^2 + C_3C_4y_1y_2\sqrt{\kappa_1\kappa_2}E_LE_{i2}\left(e^{-\frac{\alpha L}{2} - jk_n\frac{L}{2}}\right)^3}{1 - C_1C_2y_1y_2E_L\left(e^{-\frac{\alpha L}{2} - jk_n\frac{L}{2}}\right)^2}\right] \tag{9}$$

$$E_{t2} = C_2 y_2 E_{i2} + \left[\frac{C_1 C_2 \kappa_1 \sqrt{\kappa_1 \kappa_2} E_L E_{i1} e^{-\frac{\alpha L}{2} - jkn\frac{L}{2}} + C_1 C_3 y_1 y_2 \sqrt{\kappa_2} E_L E_{i2} \left(e^{-\frac{\alpha L}{2} - jk_n \frac{L}{2}} \right)^2}{1 - C_1 C_2 y_1 y_2 E_L \left(e^{-\frac{\alpha L}{2} - jk_n \frac{L}{2}} \right)^2} \right] \tag{10}$$

Here, $C_1 = \sqrt{1-\gamma_1}$, $C_2 = \sqrt{1-\gamma_2}$, $C_3 = 1-\gamma_1$, $C_4 = 1-\gamma_2$, $y_1 = \sqrt{1-\kappa_1}$ and $y_2 = \sqrt{1-\kappa_2}$.

E_{t1} and E_{t2} represent optical fields of the throughput and drop ports, respectively. The chaotic noise cancellation can be managed by using the specific parameters of the centred ring, in which required signals can be retrieved by specific users.

3. RESULTS AND DISCUSSION

To simulate the results on the basis of the security and capacity of optical soliton communication, MATLAB (MathWorks, Natick, MA, USA) software was used. Programming codes were written in regard to the ring resonator parameters, namely the coupling coefficient, ring radius, central wavelength, linear and nonlinear refractive indices, linear and nonlinear phase, round trips, internal loss and so forth. Actual data from practical experiments were implemented for simulation programming codes for different input pulses propagating inside the nonlinear Kerr type fibre ring resonators. In operation, a dark soliton pulse with a maximum power of 2 W was input into the system, in which the Gaussian beam has a power of 700 mW. The ring radii were $R_{ad} = 15$ μm and $R_L = 6$ μm. The coupling coefficients of the centred ring resonator were given by $\kappa_1 = 0.12$ and $\kappa_2 = 0.35$, where the coupling coefficient of the left ring was $\kappa_3 = 0.5$. The selected fixed parameters of the system ranged from $\lambda_0 = 1.55\,\mu m$ to $n_0 = 3.34$ (InGaAsP/InP). The effective core areas ranged from $A_{eff} = 0.50$ to $0.10\,\mu m^2$. The waveguide and coupling loses were $\alpha = 0.5\,dB\,mm^{-1}$ and $\gamma = 0.1$, respectively, where the nonlinear refractive index was $n_2 = 2.2 \times 10^{-17}\,m^2\,W^{-1}$.

After the Gaussian pulse was added into the system via the add port, a dark Gaussian soliton collision was seen, in which optical tweezers in the form of valleys or potential wells could be generated. The potential well depth could be changed when it was modulated by the trapping of energy (dark Gaussian solitons interaction).

Therefore, the generated optical pulses can be used for optical communication, in which the capacity of the output signals can be improved through the generation of peaks with a smaller FWHM, as shown in Figure 2. Figure 2(a) shows the input dark soliton and Gaussian pulse with a central wavelength of $\lambda_0 = 1.55$ μm. Figure 2(b)–(d) shows the amplified interior potential well signals, whereas the

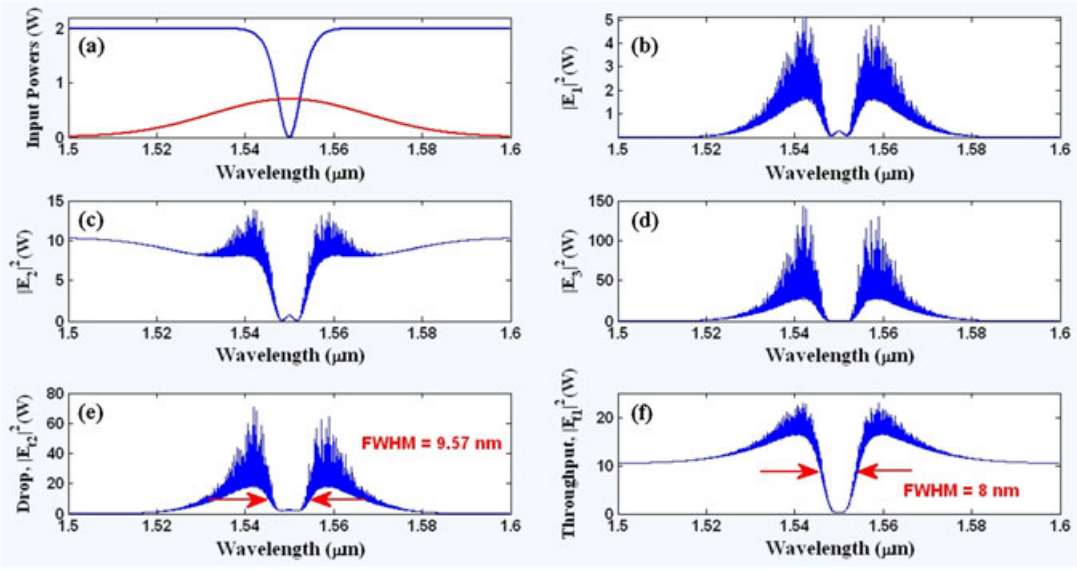

Figure 2. Results of the potential wells generation: (a) input dark soliton and Gaussian pulse; (b)–(d) interior amplified signals; (e) and (f) drop and through port output signals with full-width half-maximum (FWHM) of 9.57 and 8 nm, respectively, where $\kappa_1 = 0.12$, $\kappa_2 = 0.35$ and $\kappa_3 = 0.5$.

Security Comm. Networks 2013; **6**:1301–1309 © 2013 John Wiley & Sons, Ltd.
DOI: 10.1002/sec

sharp pulse with an FWHM of 8 and 9.57 nm can be seen in Figure 2(e) and (f) for the drop and through port output signals, respectively.

In order to improve the system, narrower soliton pulses are recommended where the attenuation of such signals during transmission become less compared with conventional peaks of micrometre laser pulses. Selected parameters of the system are fixed to $\lambda_0 = 1.55\,\mu m$ and $n_0 = 3.34$, and the nonlinear refractive index is $n_2 = 1.3 \times 10^{-17}\,m^2\,W^{-1}$. The waveguide and coupling loses are $\alpha = 0.5\,dBmm^{-1}$ and $\gamma = 0.1$, respectively. The ring radii are $R_{ad} = 10\,\mu m$ and $R_L = 3\,\mu m$, and the coupling coefficients are $\kappa_1 = 0.35$, $\kappa_2 = 0.1$ and $\kappa_3 = 0.95$, where the optical tweezers can be generated at the central wavelength $\lambda_0 = 1.55\,\mu m$ shown in Figure 3. Figure 3(a) shows the input dark soliton and Gaussian pulse with the same power of 1 W. Figure 3 (b)–(d) shows the interior and amplified signals within the system where the output signals at the drop and through ports are shown in Figure 3(e) and (f), respectively.

To obtain high-capacity transmission of generated optical tweezers, multiple input optical dark solitons and Gaussian pulse with powers of 2 and 1 W can be inserted into the system, respectively. The ring resonator is connected to the add/drop ring with radius $R_L = 10\,\mu m$ and coupling coefficient $\kappa_3 = 0.5$. The effective area of the coupling section is $A_{eff} = 25\,\mu m^2$. The optical add/drop ring has radius of $R_{ad} = 15\,\mu m$ where the coupling coefficients are $\kappa_1 = 0.35$ and $\kappa_2 = 0.25$. The dark solitons are propagating inside the system with central wavelengths of $\lambda_0 = 1.45$, 1.50 and $1.55\,\mu m$. Figure 4(a) shows the optical inputs in the form of dark solitons and Gaussian pulse. The nonlinear condition forms the interior signals as chaotic signals respect to 20 000 roundtrips of the input powers. The linear and nonlinear refractive indices of the medium are fixed to $n_0 = 3.34$ and $n_2 = 2.5 \times 10^{-17}$. By adjusting the parameters such as the dark and Gaussian powers at the input and add ports and the coupling coefficients, the tweezers depth would be controlled and tuned as shown in Figure 4(b)–(d). Amplification of the signals occurs within the nonlinear system, which makes the signals suitable for long-distance communication. Smallest tweezers width of 4.2 nm is generated at the through port shown in Figure 4(e), where Figure 4(f) shows the drop port potential wells with FWHM of 18.5 nm.

The proposed transmission unit is a quantum processing system that can be used to generate a high-capacity packet of quantum codes within the series of MRRs in which the cloning unit is operated by the add/drop filter (R_{dN1}) shown in Figure 5 [23]. A high data capacity can be applied through the use of more wavelength carriers that are provided by the transmission unit system.

In operation, the computing data can be modulated and input into the system via a receiver unit that is encoded to the quantum signal processing system shown in Figure 6 [24]. The receiver unit can be used to generate quantum bits using a polarizing beam splitter.

Figure 6 shows two pairs of possible polarization-entangled photon generation within the MRR device, which have four polarization orientation angles: 0°, 90°, 135° and 180°. It can be implemented by using the optical component, called a polarization rotatable device, and the polarizing beam splitter. Each pair of the transmitted qubits can form by itself the entangled photon pair. A polarization coupler separates the basic vertical and horizontal polarization states. The horizontally polarized pulses have a temporal separation of Δt. The coherence time of the consecutive pulses is greater than Δt. Then, the following state is created by Equation (11) [25]:

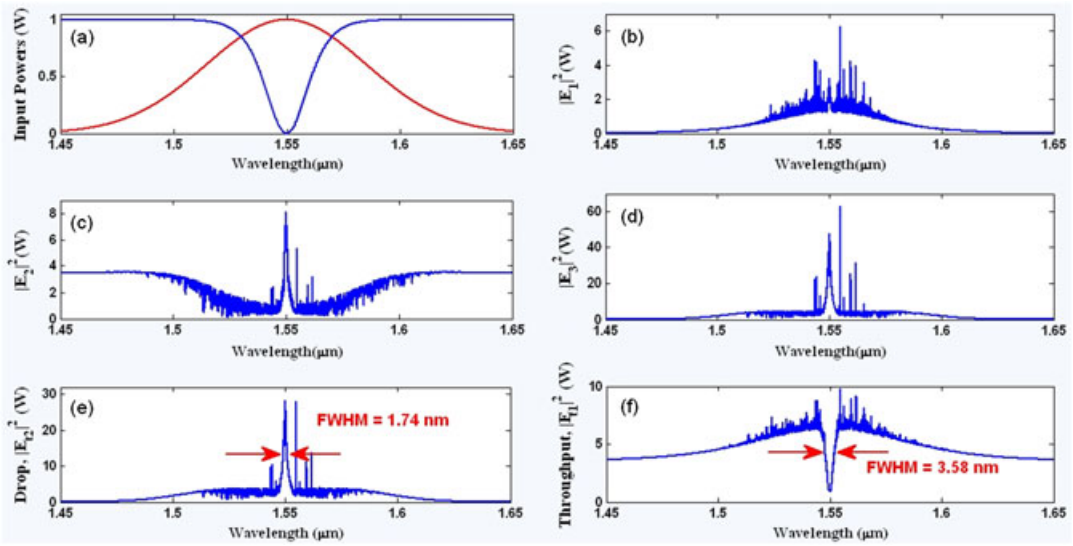

Figure 3. Results of the optical tweezers generation: (a) input dark soliton and Gaussian pulse; (b)–(d) interior amplified signals; (e) and (f) drop and through port output signals with full-width half-maximum (FWHM) of 1.74 and 3.58 nm, respectively, where $\kappa_1 = 0.35$, $\kappa_2 = 0.1$ and $\kappa_3 = 0.95$.

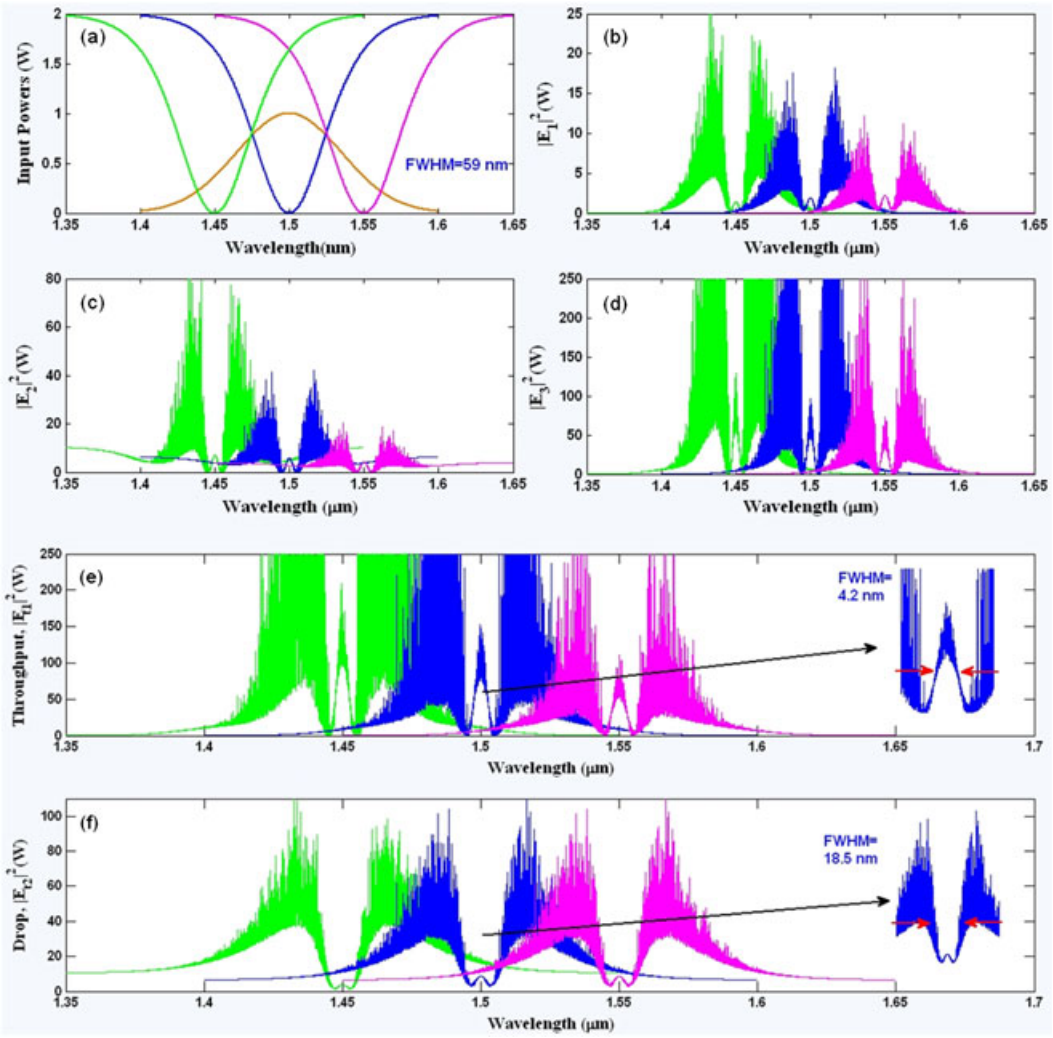

Figure 4. Optical tweezers generation within the system: (a) input of optical dark solitons and Gaussian pulse; (b)–(d) amplified and tuned optical signals; (e) optical tweezers output with full-width half-maximum (FWHM) = 4.2 nm; (f) potential wells output with FWHM = 18.5 nm.

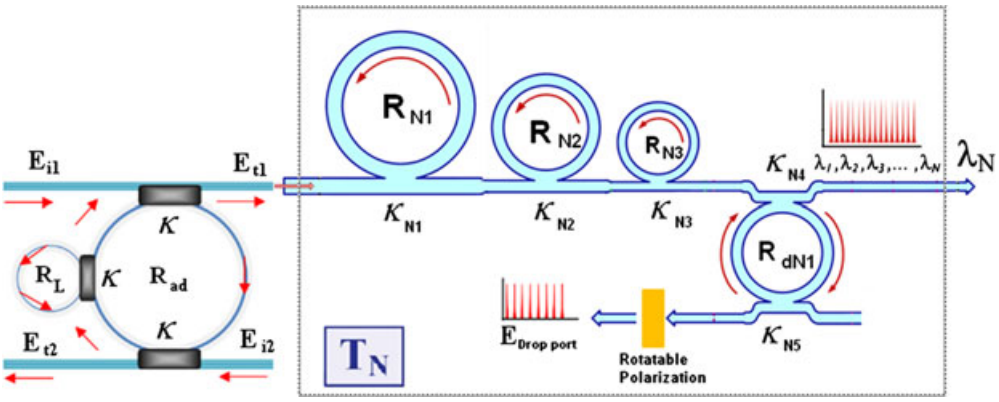

Figure 5. A schematic of the quantum tweezers manipulation within a ring resonator at the transmission unit (T_N): R_{NS}, ring radii; κ_{NS}, coupling coefficients; R_{dNS}, an add/drop ring radius.

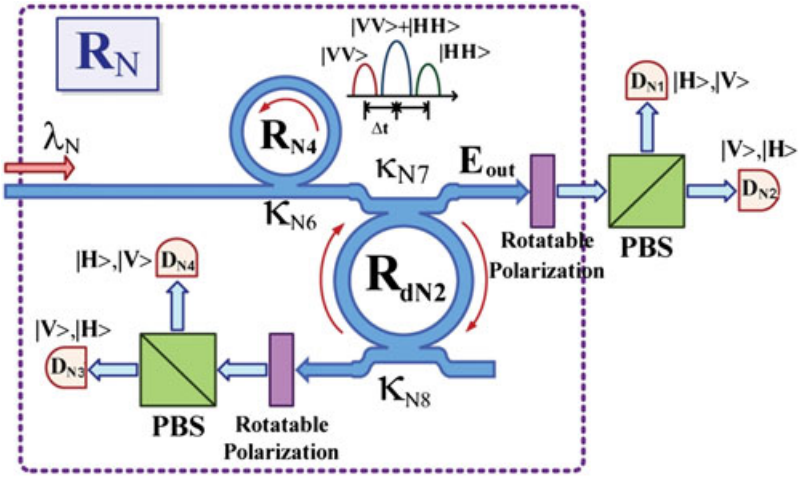

Figure 6. A schematic of an entangled photon pair manipulation within a ring resonator. The quantum state is propagating to a rotatable polarizer and then is split by a polarizing beam splitter (PBS) flying to detector D_{N1}, D_{N2}, D_{N3} and D_{N4}.

$$|\Phi>_p = |1,H>_s|1,H>_i + |2,H>_s|2,H>_i \qquad (11)$$

Here, T is the number of time slots (1 or 2), which denotes the state of polarization (horizontal |H> or vertical |V>). The subscript identifies whether the state is in the signal (s) or the idler (i) state. This two-photon state with |H> polarization shown by Equation (11) is input into the orthogonal polarization-delay circuit. The delay circuit consists of a coupler, and the difference between the round-trip times of the MRR is equal to Δt. The delay circuit converts |k, H> into

$$r|k,\mathrm{H}> + t_2\exp(i\Phi)|k+1, \mathrm{V}> + rt_2\exp(i_2\Phi)|k+2,\mathrm{H}> + r_2t_2\exp(i_3\Phi)|k+3,\mathrm{V}>$$

where t and r are the amplitude transmittances to cross and bar ports in a coupler. Equation (11) is converted into the polarized state by the delay circuit as

$$\begin{aligned}|\Phi> = &|[1,H>_s + \exp(i\Phi_s)|2,V>_s] \\ &\times[|1,H>_i + \exp(i\Phi_i)|2,V>_i] \\ &+[|2,H>_s + \exp(i\Phi_s)|3,V>_s \\ &\times[|2,H>_i + \exp(i\Phi_i)|2,V>_i =] \\ &[|1,H>_s|1,H>_i + \exp(i\Phi_i)|1,H>_s|2,V>_i] \\ &+\exp(i\Phi_s)|2,V>_s|1,H>_i \\ &+\exp[i(\Phi_s+\Phi_i)]|2,V>_s|2,V>_i + |2,H>_s|2,H>_i \\ &+\exp(i\Phi_i)|2,H>_s|3,V>_i + \exp(i\Phi_s)|3,V>_s|2,H>_i \\ &+\exp[i(\Phi_s+\Phi_i)]|3,V>_s|3,V>_i\end{aligned} \qquad (12)$$

By the coincidence that occurs in the second time slot, we can extract the fourth and fifth terms. As a result, we can obtain the following polarization-entangled state:

$$|\Phi> = |2,H>_s|2,H>_i + \exp[i(\Phi_s+\Phi_i)]|2,V>_s|2,V>_i \qquad (13)$$

The response time of the Kerr effect is assumed to be much less than the cavity round-trip time. Because of the Kerr nonlinearity type, the strong pulses acquire an intensity-dependent phase shift during propagation. The interference of light pulses at the coupler introduces the entangled output beam. The polarization states of light pulses are changed and converted during the circulation in the delay circuit, leading to the formation of the polarization-entangled photon pairs. The entangled photons of the nonlinear ring resonator are then separated into signal and idler photon probabilities. The polarization angle adjustment device is applied to investigate the orientation and optical output intensity.

The transporter states can be controlled and identified using the quantum processing system, as shown in Figures 5 and 6. In operation, the encoded quantum secret codes can be input into the network system via a TDMA system. The schematic of the TDMA system is shown in Figure 7, in which quantum cryptography for communication networks can be obtained. Therefore, transportation of quantum codes can be performed, where different signal information propagates in the network communication via a TDMA transmission system. This system uses data in the form of secured quantum codes to be transferred to single users via different lengths of the fibre optics line to the TDMA transmitter.

Therefore, some digital code information can be shared between users in different time slots. The transmission unit is a part of the quantum processing system that can be used to transfer the high-capacity packet of quantum codes. Moreover, a large amount of data can be transferred by using more wavelength carriers.

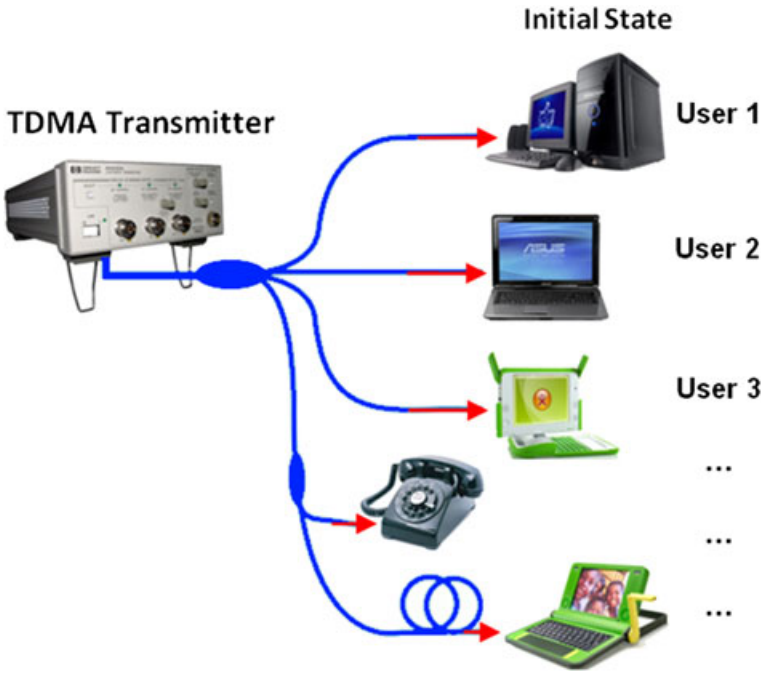

Figure 7. Schematic of the time division multiple access (TDMA) system.

4. CONCLUSION

The novel system of quantum code generation for secured optical communication has been demonstrated. Optical tweezers in the form of potential well signals are generated by the dark soliton propagating in an MRR. Narrow optical tweezers pulses with an FWHM of 3.58, 4.2 and 8 nm are generated at the through port of the PANDA ring resonator system. Tweezers with FWHM of 1.74, 9.57 and 18.5 nm could be generated at the drop port of the system. The quantum signal processing unit is connected to the potential well pulses, which can be used to generate qubits, thus providing a secure and high-capacity transmission of data. This secured code information can be used in a communication link via a TDMA system, which provides the transmission of quantum codes to different users in different time slots.

ACKNOWLEDGEMENT

I. S. Amiri would like to thank UTM for providing the research facilities.

REFERENCES

1. Konishi T, Itoh R, Itoh K. Wavelength- and time-selective reconfigurable optical add/drop multiplexer using time-frequency domain processing. *EURASIP Journal on Advances in Signal Processing* 2010; **2010**:1.
2. Kabakova IV, de Sterke CM, Eggleton BJ. Bistable switching and reshaping of optical pulses in a Bragg grating cavity. *JOSA B* 2010; **27**:12. 2648–2653.
3. Uomwech K, Sarapat K, Yupapin P. Dynamic modulated Gaussian pulse propagation within the double PANDA ring resonator system. *Microwave and Optical Technology Letters* 2010; **52**:8. 1818–1821.
4. Tamee K, Srinuanjan K, Mitatha S, Yupapin P. Distributed Sensors using a PANDA ring resonator type in multi wavelength router. *Sensors Journal, IEEE* 2011:99. 1–1.
5. Amiri IS, Afroozeh A, Bahadoran M. Simulation and analysis of multisoliton generation using a PANDA ring resonator system. *Chinese Physics Letters* 2011; **28**:104205.
6. Juan ML, Righini M, Quidant R. Plasmon nano-optical tweezers. *Nature Photonics* 2011; **5**:6. 349–356.
7. Vossen DLJ, van der Horst A, Dogterom M, van Blaaderen A. Optical tweezers and confocal microscopy for simultaneous three-dimensional manipulation and imaging in concentrated colloidal dispersions. *Review of Scientific Instruments* 2004; **75**:9. 2960–2970.
8. França V, Prataviera G. Stability and entanglement in optical-atomic amplification of trapped atoms: the role of atomic collisions. *Physical Review A* 2007; **75**:4. 043604.
9. He J, Yang B, Zhang T, Wang J. Efficient extension of the trapping lifetime of single atoms in an optical tweezer by laser cooling. *Physica Scripta* 2011; **84**:025302.

10. Shibayama E, Yonezawa A. Secure software infrastructure in the Internet age. *New Generation Computing* 2003; **21**:2. 87–106.
11. Yupapin P, Thongmee S, Sarapat K. Second-harmonic generation via micro ring resonators for optimum entangled photon visibility. *Optik—International Journal for Light and Electron Optics* 2010; **121**:7. 599–603.
12. Pornsuwanchroen N, Jamsai M, Yupapin P. QKD and QDC via optical–wireless link for quantum mobile telephone network application. *Optik—International Journal for Light and Electron Optics* 2010; **121**:12. 1123–1128.
13. Xu J, Chen HW, Liu WJ, Liu ZH. Selection of unitary operations in quantum secret sharing without entanglement. *SCIENCE CHINA Information Sciences* 2011; **54**:9. 1837–1842.
14. Yooplao P, Pongwongtragull P, Mitatha S, Yupapin P. Crosstalk effects of quantum key distribution via a quantum router. *Microwave and Optical Technology Letters* 2011; **53**:5. 1094–1099.
15. Wang LG, Chai HS. Revisit on dynamic radiation forces induced by pulsed Gaussian beams. *Optics Express* 2011; **19**:15. 14389–14402.
16. Becker C, Stellmer S, Soltan-Panahi P, *et al*. Oscillations and interactions of dark and dark–bright solitons in Bose–Einstein condensates. *Nature Physics* 2008; **4**:6. 496–501.
17. Suwanpayak N, Teeka C, Yupapin PP. Hybrid transistor manipulation controlled by light. *Microwave and Optical Technology Letters* 2011; **53**:11. 2533–2537.
18. Amiri IS, Afroozeh A, Bahadoran M. Simulation and analysis of multisoliton generation using a PANDA ring resonator system. *Chinese Physics Letters* 2011; **28**:104205.
19. Amiri IS, Ali J, Yupapin P. Enhancement of FSR and finesse using add/drop filter and PANDA ring resonator systems. *International Journal of Modern Physics B* 2012; **26**:04.
20. Manipatruni S, Chen L, Lipson M. Ultra high bandwidth WDM using silicon microring modulators. *Optics Express* 2010; **18**:16. 16858–16867.
21. Bradley JDB, Pollnau M. Erbium-doped integrated waveguide amplifiers and lasers. *Laser & Photonics Reviews* 2011; **5**:3. 368–403.
22. Mitatha S, Pornsuwancharoen N, Yupapin P. A simultaneous short-wave and millimeter-wave generation using a soliton pulse within a nano-waveguide. *Photonics Technology Letters, IEEE* 2009; **21**:13. 932–934.
23. Threepak T, Mitatha S, Luangvilay X, Yupapin P. Quantum cryptography via a wavelength router for Internet security. *Microwave and Optical Technology Letters* 2010; **52**:11. 2505–2509.
24. Erven C, Couteau C, Laflamme R, Weihs G. Entangled quantum key distribution over two free-space optical links. *Optics Express* 2008; **16**:21. 16840–16853.
25. Suchat S, Khunnam W, Yupapin PP. Quantum key distribution via an optical wireless communication link for telephone networks. *Optical Engineering* 2007; **46**:100502.